Astron. Astrophys. 334, L41–L44 (1998)

ASTRONOMY AND ASTROPHYSICS

LETTER

Letter to the Editor

Detection of methyl radicals (CH_3) on Saturn⋆

B. Bézard[1], **H. Feuchtgruber**[2], **J.I. Moses**[3], **and T. Encrenaz**[1]

[1] DESPA, Observatoire de Paris, F-92195 Meudon, France
[2] Max-Planck-Institut für Extraterrestrische Physik, D-85748 Garching, Germany
[3] Lunar and Planetary Institute, Houston, TX 77058–1113, USA

Received 23 March 1998 / Accepted 20 April 1998

Abstract. We report the first detection of methyl radicals (CH_3) in the upper atmosphere of Saturn. Emission from the ν_2 Q–branch of CH_3 at 16.50 μm was detected from observations with the Short–Wavelength Spectrometer of the ISO satellite. A CH_3 column density in the range 1.5–7.5$\times10^{13}$ molec cm^{-2} is derived, taking into account uncertainties in the data calibration, CH_3 band strength, and atmospheric model. Results are compared with predictions of photochemical models. The CH_3 abundance is mostly sensitive to the poorly known methyl recombination rates and to the eddy mixing profile. The ISO observations imply either CH_3 recombination rates larger than used in current photochemical models, or an eddy mixing coefficient near the methane homopause smaller than inferred from Voyager ultraviolet measurements.

Key words: Planets and satellites: Saturn – infrared: solar system

1. Introduction

Methane photochemistry in the atmospheres of the giant planets leads to the formation of heavier hydrocarbons and may be a source of stratospheric hazes. Ethane (C_2H_6) and acetylene (C_2H_2) are the most abundant products in all giant planets. On Saturn, two higher-order hydrocarbons (methyl-acetylene CH_3C_2H, and diacetylene C_4H_2) have recently been detected with the Short-Wavelength Spectrometer (SWS) of the ISO satellite (de Graauw et al. 1997). Hydrocarbon photochemistry is initiated by the photodissociation of methane in the homopause region, leading to the production of CH, CH_2, and CH_3 radicals (Mordaunt et al. 1993). Ethylene is formed via pathways involving CH insertion into CH_4, and ethane is produced by the reaction $2CH_3 \xrightarrow{M} C_2H_6$. Acetylene and heavier hydrocarbons are subsequently manufactured through reaction schemes of various complexity (e.g. Gladstone et al. 1996; Romani et al. 1993).

The importance of the methyl radical (CH_3) as an intermediate in the hydrocarbon photochemistry prompted us to search for its presence in Saturn and Neptune. The ν_2 band of CH_3, centered at 16.50 μm, is very strong ($\sim$2.5$\times10^{-17}$ cm molec^{-1}, Wormhoudt and McCurdy 1989), but it is not observable from the ground. We then used the Short-Wavelength Spectrometer of the ISO satellite to search for this compound and we report here its first detection on Saturn. The Neptune observations will be described elsewhere.

2. Observations

Observations of Saturn in the 16.42–16.58 μm range were carried out on 30 December 1997 UT using the grating mode of the SWS (AOT 02). The spectrum was recorded at a resolving power of 1700. The total observing time was 37 min. Descriptions of the ISO satellite and of the SWS spectrometer can be found in Kessler et al. (1996) and de Graauw et al. (1996) respectively. The aperture ($14''\times27''$at half maximum) was centered on Saturn's disk with the long axis oriented along the celestial north. Saturn's equatorial diameter was $18''$, slightly larger than the slit width. The sub-Earth latitude was -11°. The accuracy of the absolute flux scale is estimated to $\approx$20%. Instrumental fringing was removed by fitting the detector relative response function (RSRF) to the fringes of the observation before dividing it out. The correction was mostly successful although some weak residual fringing is still present. Raw data were rebinned to a resolution of 4000. The rms noise level is then about 2 Jy per resolution element. The observed spectrum is shown in Fig. 1.

The spectrum clearly shows a 50–Jy emission feature at 16.497 μm corresponding to the superposition of the Q(1,1), Q(2,2), Q(3,3), and Q(4,4) lines from the ν_2 band of CH_3. A weaker feature near 16.472 μm due to the Q(6,6) transition is also marginally detected.

3. Radiative transfer analysis

Synthetic spectra were generated from a line-by-line radiative transfer program which includes the H_2-He collision-induced

Send offprint requests to: B. Bézard (Bruno.Bezard@obspm.fr)

⋆ Based on observations with ISO, an ESA project with instruments funded by ESA Member States (especially the PI countries: France, Germany, the Netherlands and the United Kingdom) with the participation of NASA and ISAS. The SWS instrument is a joint project of the SRON and the MPE

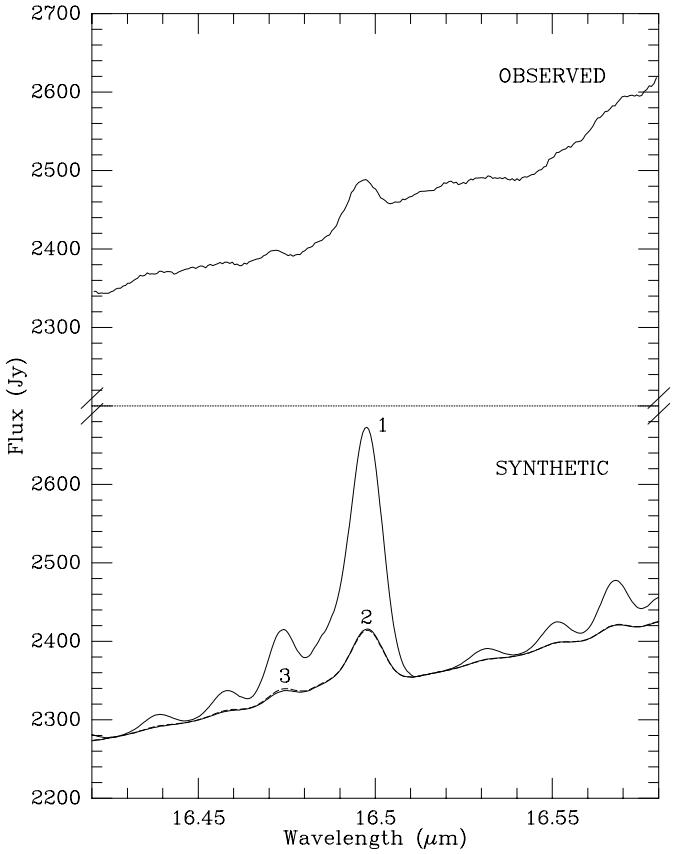

Fig. 1. Observed spectrum of the CH_3 ν_2 band on Saturn and synthetic spectra based on the atmospheric models of Fig. 2

absorption and molecular opacity from the ν_2 band of CH_3. As no line compilation existed for this compound in the available databases, we generated a line list from the standard formulation for parallel bands of symmetric top molecules. We used the molecular constants derived by Yamada et al. (1989) and the band strength measured by Wormhoudt and McCurdy (1989). We adopted a Lorentz halfwidth of 0.035 cm^{-1} atm^{-1} (Robinson et al. 1996) varying as $T^{-0.75}$.

Spectral radiances were calculated for disk-averaged conditions. They were then converted to fluxes considering that Saturn's disk was filling in 48% of the SWS field of view and adding 20 Jy to account for the ring emission at ∼70 K (4% of the field of view).

3.1. Atmospheric model

Our nominal temperature profile (Fig. 2) is based on the recent analysis of the 28 Sgr occultation data by Hubbard et al. (1997). We adopted their best fit profile above the 20-μbar level, after smoothing it in the 0.5-20 μbar pressure interval – the region directly probed by the stellar occultation data. At pressure levels less than 0.5 μbar, Hubbard et al.'s profile smoothly joins the profile derived from Voyager ultraviolet occultation data (Smith et al. 1983) which was retained only above the 0.01-μbar level. Below the 20-μbar level, we slightly modified Hubbard et al.'s profile (primarily based on the Voyager radio-occultation data, Lindal et al. 1985) to reproduce the ISO observations of Saturn's disk in the range 7-16 μm (de Graauw et al. 1997). Our profile is thus cooler around the 2-mbar region to reproduce the emission in the ν_4 band of CH_4 in the 7- to 8-μm range (originating from the 0.15-5 mbar region). It is warmer by a few degrees below the ∼20-mbar level to fit the H_2-He continuum longward of 13 μm.

This atmospheric model yields a continuum level around the CH_3 feature which is only 4% weaker than the observed value, well within the calibration uncertainty.

The CH_3 emission is optically thin; it is thus roughly proportional to the CH_3 density but depends on the temperature levels where methyl is present. Its concentration is predicted to be maximum around the methane homopause whose location depends on the eddy mixing coefficient (K) profile. To derive constraints on the column abundance, we considered vertical profiles derived from photochemical calculations (Moses et al. 1998). Fig. 2 shows the set of CH_3 profiles that have been tested in the synthetic calculations. Distribution 1 is our nominal case. Profile 2 corresponds to a lower K profile while Profile 3 is based on a larger CH_3 recombination rate (see Sect. 4 for a full description).

3.2. Determination of the CH_3 column density

Spectra generated with our nominal temperature profile and the CH_3 photochemical distributions are shown in Fig. 1. To determine the CH_3 abundance implied by the observations, we multiplied the profiles by a constant factor allowing us to match the intensity of the 16.497-μm feature. We found column densities for these rescaled profiles in the range 2.5-5$\times10^{13}$ cm^{-2}, with a peak mixing ratio between 0.8 and 2.5$\times10^{-7}$ located near the methane homopause.

These numbers are subject to uncertainties in the flux calibration of the ISO spectra (±20%) and in the strength of the ν_2 band (±30%, Wormhoudt and McCurdy 1989).

The main error source however derives from uncertainties in the thermal profile. In the 0.15-5 mbar range, it amounts to about ±2 K as a result of the 20% calibration uncertainty in the CH_4 ν_4 band. In the region probed by the 28 Sgr occultation, we assumed a 3 K error at 20 μbar regularly increasing to 6 K at 0.5 μbar, i.e. 1 and 2 times the "probable"error quoted by Hubbard et al. (1997). Above the 0.01-μbar level, where the Voyager Ultraviolet Spectrometer (UVS) profile is used, we retained the ±30 K uncertainty estimated by Smith et al. (1983). In the intermediate regions, we interpolated the error bars. We then designed a "cold" and a "hot" profile, departing from the nominal one (Fig. 2) by the above quantities. Calculations with these two profiles indicate that the CH_3 emission varies by $^{+45}_{-35}$% for Distribution 1, ±20% for Distribution 2, and ±30% for Distribution 3. We also considered another "cold" profile based on the Voyager UVS observations (Smith et al. 1983), in which the ∼140-K isothermal part extends up to the 0.025-μbar level (Fig. 2). This profile yields an emission that is 45% lower with Distribution 1, 30% lower with Distribution 3, and almost unaf-

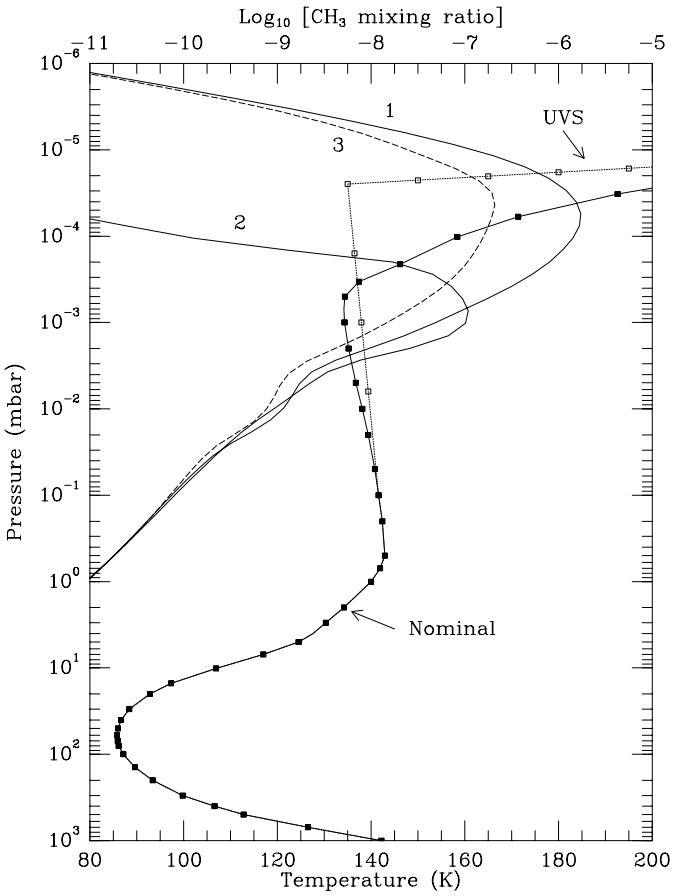

Fig. 2. Atmospheric model used for analyzing the ISO observations. The nominal temperature profile is based on the 28 Sgr occultation data (Hubbard et al. 1997). Also shown is the profile derived from Voyager UVS measurements (Smith et al. 1983). Various CH_3 mixing ratio profiles generated from photochemical calculations (1, 2, 3) [see text] were tested: Profiles 1 and 3 assume $K_h = 6\times10^7$ cm^2 s^{-1}, and Profile 2 $K_h = 7\times10^5$ cm^2 s^{-1}

fected when Distribution 2 is used. Although not consistent with Hubbard et al.'s (1997) occultation measurements, it provides an alternate choice for the temperature profile above the μbar region.

Combining the various error bars, we conclude that the CH_3 column density is located in the range 1.5-7.5$\times10^{13}$ molec cm^{-2}.

4. Comparison with photochemical models

Methyl radicals are produced both directly and indirectly from methane photolysis. Although the relative importance of the different CH_4 photodissociation pathways are not yet precisely determined, recent studies suggest that for each solar H Lyα photon absorbed by a methane molecule, the $CH_4 \xrightarrow{h\nu} CH_3$ + H pathway occurs roughly half the time (Mordaunt et al. 1993; Heck et al. 1996). The other methane photolysis products (i.e., CH_2 ($\tilde{a}\,^1A_1$), CH_2 ($\tilde{X}\,^3B_1$), and CH) can react with atmospheric H_2, H, or CH_4 to indirectly produce CH_3 through various reaction schemes (e.g. Gladstone et al. 1996; Romani et al. 1993). The primary methyl loss processes are the radical-radical combination reactions $2CH_3 \xrightarrow{M} C_2H_6$ and CH_3 + H $\xrightarrow{M}$ CH_4. These reactions, requiring a collision with a third body to stabilize the molecular product, are more effective at high atmospheric pressures. Their kinetic rates have not been measured at the low temperatures ($\sim$140 K) typical of Saturn's stratosphere; the room-temperature rates are also somewhat uncertain.

The methyl abundance is most sensitive to (1) the altitude of methane photolysis, which in turn depends on the eddy diffusion coefficient profile, and to (2) the adopted rate coefficients for the CH_3 combination reactions. The higher the altitude at which methane photolyzes, the less efficient the combination reactions are at removing CH_3, so the greater the CH_3 column abundance can be built.

Moses et al. (1998) recently developed a photochemical model that reproduces both the Voyager UVS observations of CH_4 at high altitudes (Festou & Atreya 1982; Smith et al. 1983) and the ISO observations of C_2H_2, C_2H_6, CH_3C_2H, and C_4H_2 in the lower stratosphere (de Graauw et al. 1997). In this model, the eddy mixing coefficient at the methane homopause (K_h), located near 0.01 μbar, reaches 6×10^7 cm^2 s^{-1}. This value seems to be consistent with Voyager UVS measurements of the H Lyα and the He 584 Å dayglow emissions although values as low as 5×10^6 cm^2 s^{-1} (Smith et al. 1983) and as high as 10^9 cm^2 s^{-1} (Parkinson et al. 1997) have been reported. The CH_3 profile predicted by this model (Distribution 1) overestimates the observed CH_3 emission by a factor of $\sim$6 (Fig. 1). This discrepancy is well beyond our spectral modeling uncertainties (Sect. 3). The disk-averaged temperature profile may be, to some extent, colder than in the -15 to 6° latitude regions probed by the 28 Sgr occultation lightcurves. However, a 40-K decrease in the 0.1-1-μbar region would be required to solve the discrepancy, a huge variation that we regard as possible but unlikely.

Distribution 2 (Fig. 2) derives from a case in which K_h is decreased to 7×10^5 cm^2 s^{-1}. The homopause is accordingly located at deeper levels, around 0.3 μbar. This model no longer fits the UVS observations of CH_4 but yields a CH_3 emission within the calibration/modelling uncertainty (Fig. 1) while preserving the agreement with the other hydrocarbon bands (de Graauw et al. 1997). In this model, methane is photolyzed at higher pressure, lower temperature, levels; the resulting increase in the efficiency of the CH_3 combination reactions leads to a factor of 2.3 decrease in the methyl column abundance and a factor of 5 decrease in the emission intensity.

The above models use Slagle et al.'s (1988) expression for the temperature-dependence of the $2CH_3 \xrightarrow{M} C_2H_6$ reaction rate in the low-pressure regime. However their analytical formulation is based on laboratory measurements in the range 296-906 K and extrapolation at lower temperatures is hazardous. The 140-K reaction rate derived from Slagle et al. is $\sim3.5\times10^{-26}$ cm^6 s^{-1}. Extrapolation of another expression also derived from high-temperature measurements leads to a rate 15 times larger (MacPherson et al. 1985). Photochemical calculations run with MacPherson et al.'s expression produce a CH_3 profile (Distribution 3) with a column abundance 3.5 times lower

than in Distribution 1. The emission feature is then reproduced within calibration and modelling uncertainties (Fig. 1).

The methyl abundance is less sensitive to the downward flux of atomic H, to the details of methane photolysis, or to the assumed stratospheric temperature. For instance, an increase in the downward H atom flux from $2.5\times10^{9}\,cm^{-2}\,s^{-1}$ to $1.3\times10^{10}\,cm^{-2}\,s^{-1}$ in the model leads only to a 14% decrease in the CH_3 column abundance. Reasonable changes in the branching ratios of the CH_4 photolysis pathways lead to at most a 4% change in the CH_3 column, although such changes can have a larger effect on the abundances of C_2, C_3, and C_4 hydrocarbons.

5. Conclusions

The present ISO observations of the CH_3 ν_2 band on Saturn imply a CH_3 column density between 1.5 and $7.5\times10^{13}\,cm^{-2}$. Current photochemical models tend to overpredict the methyl abundance (e.g. Distribution 1). This quantity is sensitive to the CH_3 recombination rates which have not been measured at the low temperatures prevailing in Saturn's upper atmosphere. It is thus difficult to know if the discrepancy is merely due to this poorly known chemical rate. A CH_3-CH_3 combination rate of at least $4\times10^{-25}\,cm^{6}\,s^{-1}$ at 140 K, i.e. 10 times larger than extrapolated from Slagle et al.'s (1988) expression, would be needed to solve the issue.

If reasonable changes in these reaction rates cannot by themselves allow the models to reproduce the ISO CH_3 observations, then the eddy diffusion coefficient profile most likely needs to be reduced. Lower values of the eddy diffusion coefficient at high altitudes prevent the photochemical models from reproducing the Voyager UVS occultation results for CH_4 (Festou & Atreya 1982, Smith et al. 1983) and He emission (Parkinson et al. 1997). This inconsistency could be resolved if (1) the eddy diffusion coefficient profile changes with time, (2) if the global average diffusion profile is different from that at the UVS occultation latitudes, or (3) if the altitudes in the UVS analyses are not well constrained. It should be noted that the recent ground-based 28 Sgr occultation results (Hubbard et al. 1997) are also inconsistent with the UVS measurements. This problem clearly requires further modeling.

The present observations of the CH_3 radical appear to be a very useful diagnostic tool to constrain the eddy mixing coefficient in the homopause region, provided that the recombination rates are precisely known. We therefore strongly encourage measurements of the CH_3 + CH_3 recombination rate as a function of pressure and temperature under conditions relevant to the upper atmospheres of the giant planets.

References

de Graauw Th., Haser L.N., Beintema D.A., et al., 1996, A&A 315, L49

de Graauw Th., Feuchtgruber H., Bézard B., et al., 1997, A&A 321, L13

Festou M.C., Atreya S.K.,1982, GRL 9, 1147

Gladstone G.R., Allen M., Yung Y.L., 1996, Icarus 119, 1

Heck A.J.R., Zare R.N., Chandler D.W., 1996, J. Chem. Phys. 104, 4019

Hubbard W.B., Porco C.C., Hunten D.M., et al., 1997, Icarus 130, 404

Kessler M.F., Steinz J.A., Andreegg, M.E., et al., 1996, A&A 315, L27

Lindal G.F., Sweetnam D.N., Eshleman V.R., 1985, AJ 90, 1136

MacPherson M.T., Pilling M.J., Smith M.J.C., 1985, J. Phys. Chem. 89, 2268

Mordaunt D.H., Lambert I.R., Morley G.P., et al., 1993, J. Chem. Phys. 98, 2054

Moses J.I., Bézard B., Lellouch E., Feuchtgruber H., Allen M., 1998, Lunar Planet. Sci. 29, 1652

Parkinson C.D., Griffioen E., McConnell J.C., Gladstone G.R., Sandel B.R., 1997, BAAS 29, 995

Robinson G.N., Zahniser M.S., Freedman A., Nelson D.D. Jr., 1996, JMS 176, 337

Romani P.N., Bishop J., Bézard B., Atreya S., 1993, Icarus 106, 442

Slagle I.R., Gutman D., Davies J.W., Pilling M.J., 1988, J. Phys. Chem. 92, 2455

Smith G.R., Shemansky D.E., Holberg J.B., et al., 1983, JGR 88, 8667

Wormhoud J., McCurdy K.E., 1989, Chem. Phys. Lett. 156, 47

Yamada C., Hirota E., Kawaguchi K., 1981, J. Chem. Phys. 75, 5256